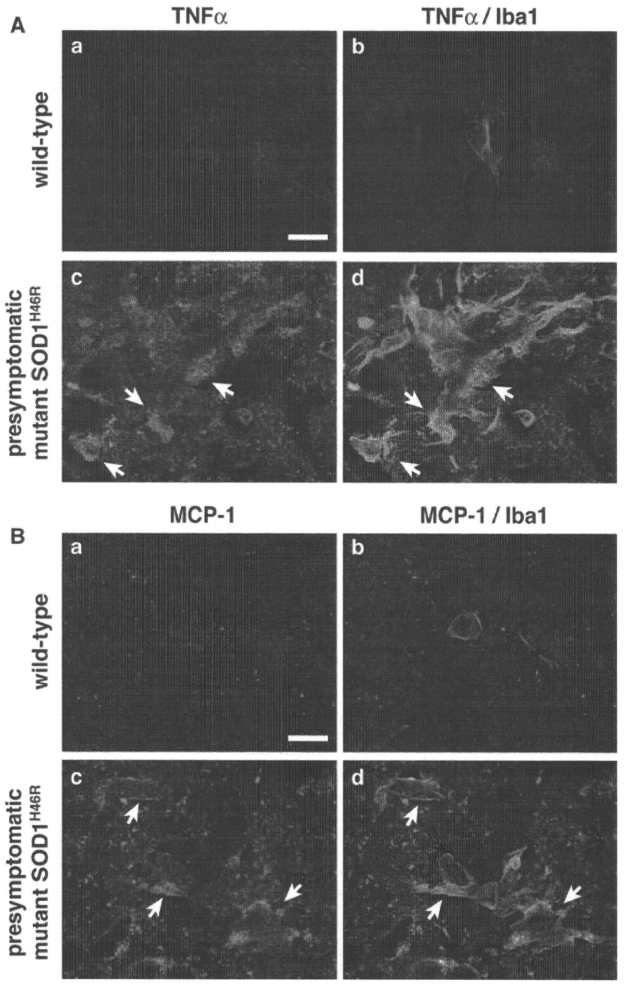

Fig. 5. Spinal cord sections of wild-type and presymptomatic mutant $SOD1^{H46R}$ rats were immunostained with anti-TNFα (green in **A**), anti-MCP-1 (green in **B**), and anti-Iba1 (red) antibodies. Microglial aggregates observed in the anterior horn of presymptomatic mutant $SOD1^{H46R}$ rats were immunoreactive for TNFα (A) and MCP-1 (B). Scale bars = 10 μm.

symptomatic mutant $SOD1^{H46R}$ rats compared with wild-type rats (Fig. 1, Supp. Info. Fig. 1B), but ChAT immunoreactivity was weaker in the motoneurons near aggregated microglia in presymptomatic mutant $SOD1^{H46R}$ rats (Fig. 2, Supp. Info. Fig. 1C). ChAT immunoreactivity has been reported to be decreased in well-preserved neurons during the early, nonadvanced stage of ALS (Kato, 1989). Previous studies have shown that motoneuronal lipid peroxidative injury occurs before the motoneuron pathology, which precedes the onset of the ultrastructural and clinical motoneuron disease (Hall et al., 1997, 1998a). We immunohistochemically confirmed that the expression of malondialdehyde, which is a marker of lipid peroxidation, was increased in the motoneurons of presymptomatic mutant $SOD1^{H46R}$ rats compared with wild-type rats (data not shown). Electron microscopy also revealed that the somata of motoneurons surrounded by aggregated microglia contained the reduced granular endoplasmic reticulum and altered nucleus (Fig. 4C). Thus, microglia might react to these neuronal changes early during ALS pathogenesis, becoming activated and forming aggregates.

We have demonstrated that the aggregated microglia observed in the lumbar spinal cord sections of presymptomatic mutant $SOD1^{H46R}$ rats were proliferative. Proliferative activity is one of the characteristic properties of activated microglia. Microglia are known to proliferate in response to macrophage colony-stimulating factor (M-CSF) and granulocyte macrophage (GM-) CSF (Giulian and Ingeman, 1988; Lee et al., 1994). The M-CSF level is reported to be elevated in the CNS of ALS patients and ALS mouse models (Henkel et al., 2004; Sargsyan et al., 2005). Therefore, in the lumbar spinal cord of presymptomatic mutant $SOD1^{H46R}$ rats, the proliferation of microglia might be induced by M-CSF, resulting in the appearance of microglial aggregates. Further studies are required to investigate whether M-CSF or any other factors induce the formation of microglial aggregates.

Our immunohistochemical and ultrastructural analyses showed that phagocytic microglia were observed in the lumbar spinal cord of presymptomatic mutant $SOD1^{H46R}$ rats. Phagocytosis by microglia is an important function for the removal of dead cells and the inhibition of content leakage from dying cells (Raivich et al., 1999; Stolzing and Grune, 2004; Neumann et al., 2009). When facial nerve neurons are damaged by the injection of toxic ricin into the facial nucleus, microglia are known to exhibit phagocytic activity in association with the removal of dead cells (Streit and Kreutzberg, 1988). On the other hand, the transection of a facial nerve does not cause neuronal cell death, and activated microglia around the facial nucleus do not exhibit any phagocytic properties (Moran and Graeber, 2004). Therefore, neuronal cell death is considered to transform microglia into phagocytic cells (Stolzing and Grune, 2004; Neumann et al., 2009). In ischemia and various neurodegenerative diseases, phagocytic microglia are thought to appear following neuronal cell loss. However, in the lumbar spinal cord sections of presymptomatic mutant $SOD1^{H46R}$ rats, the loss of motoneurons was not observed (Fig. 1A, Supp. Info. Fig. 1B), and the aggregated microglia surrounding the motoneurons exhibited phagocytic features (Figs. 3B,C, 4E). These results suggest that microglial phagocytosis occurs not only after neuronal cell death but also during the early, nonadvanced stage of neuronal cell damage.

The expression of TNFα and MCP-1 is reportedly elevated in microglia isolated from mutant $SOD1^{G93A}$ transgenic mice (Weydt et al., 2004; Sargsyan et al., 2009). We have shown that immunopositive signals for TNFα and MCP-1 were localized in the aggregated microglia (Fig. 5). In diseased CNS tissues, proinflammatory factors secreted by activated microglia are known to contribute to the regulation of microglial activation in an autocrine/paracrine manner. TNFα reportedly increases the phagocytic activity of microglia (Smith et al., 1998). Therefore, we suggest that TNFα might be involved in the transformation of activated microglia to phagocytic cells. Although the involvement of MCP-1 in the phagocytic activity of microglia is still unclear, MCP-1 has been reported to induce the chemotactic migration of microglia (Zhou et al., 2007; Deng et al., 2009). MCP-1 may regulate the recruitment of microglia to damaged neurons. In various neurodegenerative diseases, such as ALS, activated microglia are thought to influence the survival of neurons by releasing inflammatory mediators, such as nitric oxide, interleukin (IL)-1β, and IL-6 (Nakajima and Kohsaka, 2001, 2004; Sargsyan et al., 2005). TNFα has been shown to induce oxidative stress and motoneuron death in rat spinal cord (Mir et al., 2009), suggesting that TNFα might damage motoneurons and be involved in disease progression during the presymptomatic stage in ALS. On the other hand, MCP-1 is important for the recruitment of immune cells to the damaged area and reportedly provides a neuroprotective function (Eugenin et al., 2003). However, the blocking of MCP-1 function has been reported to prolong the survival of mutant SOD1 transgenic mice (Keep et al., 2001). Further studies are needed to determine whether MCP-1 has a protective or injurious effect on motoneurons during the presymptomatic stage. In the cerebrospinal fluid and CNS tissues of ALS patients and ALS animal models, various factors such as IL-6 and M-CSF have been reported to be elevated (Sargsyan et al., 2005). Therefore, further studies are needed to investigate whether these factors are expressed in aggregated microglia and whether they are involved in the promotion of motoneuronal degeneration at the presymptomatic stage.

It has been reported that the increase in activated microglia and the up-regulation of proinflammatory factors escalate in accordance with disease progression (Hall et al., 1998b; Alexianu et al., 2001; Sargsyan et al., 2005). Thus, microglia seem to play a crucial role during the late stage of disease progression. However, our results provide in vivo evidence suggesting that activated and aggregated microglia exhibit phagocytic activity and

might be involved in disease progression during the presymptomatic stage in ALS. Further studies revealing the functional properties of activated microglia during the presymptomatic stage would likely further our understanding of the role of microglia in the pathogenesis of ALS.

REFERENCES

Alexianu ME, Kozovska M, Appel SH. 2001. Immune reactivity in a mouse model of familial ALS correlates with disease progression. Neurology 57:1282–1289.

Anneser JM, Chahli C, Ince PG, Borasio GD, Shaw PJ. 2004. Glial proliferation and metabotropic glutamate receptor expression in amyotrophic lateral sclerosis. J Neuropathol Exp Neurol 63:831–840.

Aoki M, Ogasawara M, Matsubara Y, Narisawa K, Nakamura S, Itoyama Y, Abe K. 1993. Mild ALS in Japan associated with novel SOD mutation. Nat Genet 5:323–324.

Aoki M, Kato S, Nagai M, Itoyama Y. 2005. Development of a rat model of amyotrophic lateral sclerosis expressing a human SOD1 transgene. Neuropathology 25:365–370.

Beers DR, Henkel JS, Xiao Q, Zhao W, Wang J, Yen AA, Siklos L, McKercher SR, Appel SH. 2006. Wild-type microglia extend survival in PU.1 knockout mice with familial amyotrophic lateral sclerosis. Proc Natl Acad Sci U S A 103:16021–16026.

Boillee S, Vande Velde C, Cleveland DW. 2006a. ALS: a disease of motor neurons and their nonneuronal neighbors. Neuron 52:39–59.

Boillee S, Yamanaka K, Lobsiger CS, Copeland NG, Jenkins NA, Kassiotis G, Kollias G, Cleveland DW. 2006b. Onset and progression in inherited ALS determined by motor neurons and microglia. Science 312:1389–1392.

Bruijn LI, Miller TM, Cleveland DW. 2004. Unraveling the mechanisms involved in motor neuron degeneration in ALS. Annu Rev Neurosci 27:723–749.

Cereda C, Baiocchi C, Bongioanni P, Cova E, Guareschi S, Metelli MR, Rossi B, Sbalsi I, Cuccia MC, Ceroni M. 2008. TNF and sTNFR1/2 plasma levels in ALS patients. J Neuroimmunol 194:123–131.

Clement AM, Nguyen MD, Roberts EA, Garcia ML, Boillee S, Rule M, McMahon AP, Doucette W, Siwek D, Ferrante RJ, Brown RH Jr, Julien JP, Goldstein LS, Cleveland DW. 2003. Wild-type nonneuronal cells extend survival of SOD1 mutant motor neurons in ALS mice. Science 302:113–117.

Deng YY, Lu J, Ling EA, Kaur C. 2009. Monocyte chemoattractant protein-1 (MCP-1) produced via NF-kappaB signaling pathway mediates migration of amoeboid microglia in the periventricular white matter in hypoxic neonatal rats. Glia 57:604–621.

Eugenin EA, D'Aversa TG, Lopez L, Calderon TM, Berman JW. 2003. MCP-1 (CCL2) protects human neurons and astrocytes from NMDA or HIV-tat-induced apoptosis. J Neurochem 85:1299–1311.

Giulian D, Ingeman JE. 1988. Colony-stimulating factors as promoters of ameboid microglia. J Neurosci 8:4707–4717.

Hall ED, Oostveen JA, Andrus PK, Anderson DK, Thomas CE. 1997. Immunocytochemical method for investigating in vivo neuronal oxygen radical-induced lipid peroxidation. J Neurosci Methods 76:115–122.

Hall ED, Andrus PK, Oostveen JA, Fleck TJ, Gurney ME. 1998a. Relationship of oxygen radical-induced lipid peroxidative damage to disease onset and progression in a transgenic model of familial ALS. J Neurosci Res 53:66–77.

Hall ED, Oostveen JA, Gurney ME. 1998b. Relationship of microglial and astrocytic activation to disease onset and progression in a transgenic model of familial ALS. Glia 23:249–256.

Henkel JS, Engelhardt JI, Siklos L, Simpson EP, Kim SH, Pan T, Goodman JC, Siddique T, Beers DR, Appel SH. 2004. Presence of dendritic cells, MCP-1, and activated microglia/macrophages in amyotrophic lateral sclerosis spinal cord tissue. Ann Neurol 55:221–235.

Imai Y, Ibata I, Ito D, Ohsawa K, Kohsaka S. 1996. A novel gene iba1 in the major histocompatibility complex class III region encoding an EF hand protein expressed in a monocytic lineage. Biochem Biophys Res Commun 224:855–862.

Kato T. 1989. Choline acetyltransferase activities in single spinal motor neurons from patients with amyotrophic lateral sclerosis. J Neurochem 52:636–640.

Keep M, Elmer E, Fong KS, Csiszar K. 2001. Intrathecal cyclosporin prolongs survival of late-stage ALS mice. Brain Res 894:327–331.

Lee SC, Liu W, Brosnan CF, Dickson DW. 1994. GM-CSF promotes proliferation of human fetal and adult microglia in primary cultures. Glia 12:309–318.

Lino MM, Schneider C, Caroni P. 2002. Accumulation of SOD1 mutants in postnatal motoneurons does not cause motoneuron pathology or motoneuron disease. J Neurosci 22:4825–4832.

Liu Y, Hao W, Dawson A, Liu S, Fassbender K. 2009. Expression of amyotrophic lateral sclerosis-linked SOD1 mutant increases the neurotoxic potential of microglia via TLR2. J Biol Chem 284:3691–3699.

Mattiazzi M, D'Aurelio M, Gajewski CD, Martushova K, Kiaei M, Beal MF, Manfredi G. 2002. Mutated human SOD1 causes dysfunction of oxidative phosphorylation in mitochondria of transgenic mice. J Biol Chem 277:29626–29633.

Mir M, Asensio VJ, Tolosa L, Gou-Fabregas M, Soler RM, Llado J, Olmos G. 2009. Tumor necrosis factor alpha and interferon gamma cooperatively induce oxidative stress and motoneuron death in rat spinal cord embryonic explants. Neuroscience (in press).

Moran LB, Graeber MB. 2004. The facial nerve axotomy model. Brain Res Brain Res Rev 44:154–178.

Nagai M, Aoki M, Miyoshi I, Kato M, Pasinelli P, Kasai N, Brown RH Jr, Itoyama Y. 2001. Rats expressing human cytosolic copper-zinc superoxide dismutase transgenes with amyotrophic lateral sclerosis: associated mutations develop motor neuron disease. J Neurosci 21:9246–9254.

Nakajima K, Kohsaka S. 2001. Microglia: activation and their significance in the central nervous system. J Biochem 130:169–175.

Nakajima K, Kohsaka S. 2004. Microglia: neuroprotective and neurotrophic cells in the central nervous system. Curr Drug Targets Cardiovasc Haematol Disord 4:65–84.

Neumann H, Kotter MR, Franklin RJ. 2009. Debris clearance by microglia: an essential link between degeneration and regeneration. Brain 132:288–295.

Neusch C, Bahr M, Schneider-Gold C. 2007. Glia cells in amyotrophic lateral sclerosis: new clues to understanding an old disease? Muscle Nerve 35:712–724.

Peters A, Palay SL, Webster H. 1991. The fine structure of the nervous system: neurons and their supporting cells. New York: Oxford University Press.

Pramatarova A, Laganiere J, Roussel J, Brisebois K, Rouleau GA. 2001. Neuron-specific expression of mutant superoxide dismutase 1 in transgenic mice does not lead to motor impairment. J Neurosci 21:3369–3374.

Raivich G, Bohatschek M, Kloss CU, Werner A, Jones LL, Kreutzberg GW. 1999. Neuroglial activation repertoire in the injured brain: graded response, molecular mechanisms and cues to physiological function. Brain Res Brain Res Rev 30:77–105.

Rosen DR. 1993. Mutations in Cu/Zn superoxide dismutase gene are associated with familial amyotrophic lateral sclerosis. Nature 364:362.

Rosen DR, Sapp P, O'Regan J, McKenna-Yasek D, Schlumpf KS, Haines JL, Gusella JF, Horvitz HR, Brown RH Jr. 1994. Genetic linkage analysis of familial amyotrophic lateral sclerosis using human chromosome 21 microsatellite DNA markers. Am J Med Genet 51:61–69.

Sargsyan SA, Monk PN, Shaw PJ. 2005. Microglia as potential contributors to motor neuron injury in amyotrophic lateral sclerosis. Glia 51:241–253.

Sargsyan SA, Blackburn DJ, Barber SC, Monk PN, Shaw PJ. 2009. Mutant SOD1 G93A microglia have an inflammatory phenotype and elevated production of MCP-1. Neuroreport 20:1450–1455.

Saxena S, Cabuy E, Caroni P. 2009. A role for motoneuron subtype-selective ER stress in disease manifestations of FALS mice. Nat Neurosci 12:627–636.

Smith ME, van der Maesen K, Somera FP. 1998. Macrophage and microglial responses to cytokines in vitro: phagocytic activity, proteolytic enzyme release, and free radical production. J Neurosci Res 54:68–78.

Stolzing A, Grune T. 2004. Neuronal apoptotic bodies: phagocytosis and degradation by primary microglial cells. FASEB J 18:743–745.

Streit WJ, Kreutzberg GW. 1988. Response of endogenous glial cells to motor neuron degeneration induced by toxic ricin. J Comp Neurol 268:248–263.

Weydt P, Yuen EC, Ransom BR, Moller T. 2004. Increased cytotoxic potential of microglia from ALS-transgenic mice. Glia 48:179–182.

Zhou Y, Ling EA, Dheen ST. 2007. Dexamethasone suppresses monocyte chemoattractant protein-1 production via mitogen activated protein kinase phosphatase-1 dependent inhibition of Jun N-terminal kinase and p38 mitogen-activated protein kinase in activated rat microglia. J Neurochem 102:667–678.

Journal of Neurochemistry

JNC

JOURNAL OF NEUROCHEMISTRY | 2010 | 115 | 1057–1067

doi: 10.1111/j.1471-4159.2010.06996.x

Macrophage-colony stimulating factor as an inducer of microglial proliferation in axotomized rat facial nucleus

Shinichi Yamamoto,* Kazuyuki Nakajima*,† and Shinichi Kohsaka†

*Department of Bioinformatics, Faculty of Engineering, Soka University, Tokyo, Japan

†Department of Neurochemistry, National Institute of Neuroscience, Tokyo, Japan

Abstract

We analyzed the mechanism of microglial proliferation in rat axotomized facial nucleus (axotFN). In immunoblotting analysis for possible mitogens, we noticed that the amounts of macrophage-colony stimulating factor (M-CSF) increased in the axotFN for 3–7 days after transection. In contrast, the amounts of granulocyte macrophage-CSF and interleukin-3 did not significantly increase. A potential source for M-CSF was immunohistochemically verified to be microglia. Immunoblotting showed that the amounts of receptor for M-CSF (cFms) increased in the axotFN for 3–14 days after injury, and immunohistochemical staining showed that cFms is expressed in microglia. Proliferating cell nuclear antigen as a marker of proliferation was immunohistochemically identified in microglia in axotFN, and the level was found to peak 3 days after transection in immunoblotting. Hypothesizing that up-regulated M-CSF triggers the above phenomena, we investigated the effects of M-CSF on cFms and proliferating cell nuclear antigen levels in primary microglia. The biochemical experiments revealed that M-CSF induces cFms and drives the cell cycle in microglia. The neutralization of M-CSF in microglia derived from axotFN significantly reduced the proliferation. These results demonstrate that up-regulated M-CSF triggers the induction of cFms in microglia and causes the microglia to proliferate in the axotFN.

Keywords: cFms, M-CSF, microglia, PCNA, proliferation, transection of facial nerve.

J. Neurochem. (2010) **115**, 1057–1067.

Microglia are glial-type cells distributed throughout the CNS with regular spacing. Microglial cells account for 5–20% of the glial cell population in the normal adult brain (Streit 2005). Once stimulated in pathological or injured brains, including those affected by Alzheimer's disease (Dickson *et al.* 1993; McGeer *et al.* 1993; Nelson *et al.* 2002), Parkinson's disease (Członkowska *et al.* 2002), infection (Weinstein *et al.* 1990; Dickson *et al.* 1993; Nelson *et al.* 2002), inflammation (Lassmann *et al.* 1986; Gehrmann and Kreutzberg 1992; Nelson *et al.* 2002), ischemia (Kato *et al.* 2003), axotomy (Kreutzberg 1996), and trauma (Giulian *et al.* 1989), microglia are commonly activated and proliferate at the affected site. Accordingly, this proliferation is the most remarkable feature of microglia in unusual or disordered states of the CNS.

It is known that several molecules have the ability to proliferate microglia. Colony-stimulating factors such as macrophage-colony stimulating factor (M-CSF) (Giulian and Ingleman 1988; Sawada *et al.* 1990), granulocyte macrophage-colony stimulating factor (GM-CSF) (Giulian and Ingeman 1988; Ganter *et al.* 1992; Lee *et al.* 1994), and inteleukin-3 (IL-3; multiple CSF) (Giulian and Ingleman 1988; Ganter *et al.* 1992) have been shown to enhance microglial proliferation under *in vitro* conditions. IL-1 (Ganter *et al.* 1992), IL-2 (Sawada *et al.* 1995), IL-4 (Suzumura *et al.* 1993), IL-5 (Ringheim 1995; Liva and de Vellis 2001), and tumor necrosis factor-alpha (TNFα) (Ganter *et al.* 1992) have also been reported to enhance microglial proliferation. Among them, M-CSF has been highlighted as the most likely candidate for the essential mitogen of microglia *in vivo* because there is little or no microglial proliferation in the

Received April 23, 2010; revised manuscript received September 1, 2010; accepted September 3, 2010.

Address correspondence and reprint requests to Kazuyuki Nakajima, Department of Bioinformatics, Faculty of Engineering, Soka University, 1-236 Tangi-machi, Hachioji, Tokyo 192-8577, Japan.

E-mail: nakajima@t.soka.ac.jp

Abbreviations used: axotFN, axotomized facial nucleus; DMEM, Dulbecco's modified Eagle's medium; FBS, fetal bovine serum; GFAP, glial fibrillary acidic protein; GM-CSF, granulocyte macrophage-colony stimulating factor; HRP, horseradish peroxidase; Iba1, ionized Ca^{2+} binding adapter molecule 1; IL, interleukin; M-CSF, macrophage-colony stimulating factor; PBS, phosphate-buffered saline; PCNA, proliferating cell nuclear antigen; TNFα, tumor necrosis factor-alpha.

transected facial nucleus of osteopetrotic mouse that cannot produce active M-CSF (Raivich *et al.* 1994). However, the relationship between microglial proliferation and the amounts of M-CSF in the transected facial nucleus remains to be clarified, and the possibility of other mitogens being involved in the microglial proliferation must be investigated.

Therefore, in the present study, we first analyzed the levels of possible mitogens in the axotomized rat facial nucleus, focusing on the most likely mitogen M-CSF, and investigated its role in the processes of microglial proliferation.

Materials and methods

Antibodies and reagents

OX42 monoclonal antibody (CD11b) and FITC-conjugated OX42 monoclonal antibody for detecting rat complement receptor 3 were purchased from Serotec Ltd (Oxford, UK). The antibody against ionized Ca^{2+} binding adapter molecule 1 (Iba1; Imai *et al.* 1996) was obtained from Wako Pure Chemical Industries (Osaka, Japan). Santa Cruz Biotechnology (Santa Cruz, CA, USA) supplied the antibodies against actin, M-CSF, GM-CSF, IL-3, TNFα, IL-1β, and cFms. Goat anti-murine M-CSF antibody for neutralization was purchased from PeproTech (Rocky Hill, NJ, USA). This polyclonal antibody is provided as goat IgG purified by affinity chromatography. Monoclonal anti-glial fibrillary acidic protein (GFAP) antibody and polyclonal anti-GFAP polyclonal antibody were obtained from Shandon Scientific (Pittsburgh, PA, USA) and Chemicon International (Temecula, CA, USA), respectively. The antibody against proliferating cell nuclear antigen (PCNA) was purchased from Oncogene Research Products (San Diego, CA, USA).

The vectastain avidin-biotin-peroxidase complex (ABC) kit was obtained from Vector Laboratories, Inc. (Burlingame, CA, USA). Horseradish peroxidase (HRP)-conjugated goat anti-rabbit IgG was purchased from Nippon Bio-Rad lab (Tsukuba, Japan), and HRP-conjugated donkey anti-goat IgG, HRP-conjugated goat anti-mouse IgG, and rhodamine-conjugated anti-rabbit IgG were purchased from Santa Cruz. Alexa Fluor 488-conjugated anti-mouse IgG and Alexa Fluor 568-conjugated anti-rabbit IgG were purchased from Invitrogen Corporation (Carlsbad, CA, USA).

The enhanced chemiluminescence system was obtained from GE Healthcare (Buckinghamshire, UK). Mouse M-CSF, GM-CSF, IL-3, TNFα, and IL-1β were purchased from Sigma-Aldrich Japan (Tokyo, Japan). Normal goat IgG was obtained from Santa Cruz.

Transection of adult rat facial nerve

Wistar rats (8 weeks, male) were purchased from Clea Japan Inc. (Tokyo, Japan) and kept on a 12-h daylight cycle with food and water. They were cared for in accordance with the guidelines of the ethics committee of Soka University.

As one set experiment for immunohistochemical and immunoblotting studies in time course, five male rat littermates were used. The right facial nerve of the rats was transected at the stylomastoid foramen under diethylether anesthesia, as described previously (Nakajima *et al.* 1996; Graeber *et al.* 1998). These rats were decapitated at the desired time points (1, 3, 5, 7, 14 days) under anesthesia, and the whole brains were removed, frozen on dry ice, and stored at −80°C before use. At least three sets of the brains were prepared and analyzed. In sham controls, the right facial nerve was exposed at the stylomastoid foramen, but not damaged. The animals were allowed to survive for the desired time.

The brainstem was chipped from the hinder portion to the depth of the facial nucleus. The contralateral and ipsilateral facial nucleus were carefully cut out from the brainstem under frozen conditions. The cut facial nuclei were stored at −20°C until use.

Immunohistochemistry

Sections (20 μm thickness) of the brainstem were cut with a cryostat at the level of the facial nuclei (Graeber *et al.* 1998). These sections were air-dried for 20 min and fixed in 3.7% paraformaldehyde/0.1 M phosphate-buffered saline (PBS) for 5 min. Subsequently, they were treated sequentially with 5% acetone for 2 min, 100% acetone for 3 min, and 50% acetone for 2 min, and further with 0.05% Triton X-100/10 mM PBS for 5 min. These sections were blocked with blocking solution (0.2% skim milk/10 mM PBS) for 60 min at 25°C.

For visualization by diaminobenzidine, the sections were incubated with CD11b (1 : 100) or Iba1 (1 : 100) in blocking solution at 4°C overnight. After the sections were rinsed, they were incubated with biotinylated anti-mouse IgG (Vectastain ABC kit) (in case of CD11b) or biotinylated anti-rabbit IgG (in case of Iba1) for 1 h. The sections were stained with 0.001% H_2O_2 and 0.083 mM diaminobenzidine as a peroxidase substrate. The sections were dehydrated in alcohol, isopropanol, and xylene, and then mounted with Vecta Mount (Vector Laboratories).

For dual fluorescent staining, the cryosections were separately incubated with two primary antibodies at 4°C overnight, and subsequently with two fluorescent-conjugated antibodies for 3 h at 25°C. As a primary antibody, anti-M-CSF polyclonal antibody (1 : 100), FITC-conjugated CD11b monoclonal antibody (1 : 100), anti-cFms polyclonal antibody (1 : 100), anti-GFAP monoclonal antibody (1 : 200), anti-PCNA monoclonal antibody (1 : 100), anti-Iba1 polyclonal antibody (1 : 100), and anti-GFAP polyclonal antibody (1 : 500) were used. Alexa 488-conjugated anti-mouse IgG (1 : 100) and Alexa 568-conjugated anti-rabbit IgG (1 : 200) or rhodamin-conjugated anti-rabbit IgG (1 : 200) were used as secondary antibodies. The sections were dehydrated and mounted as described above, and then observed by fluorescence microscopy.

Microglia derived from explant culture of transected facial nucleus

To confirm the presence of M-CSF in microglia occurring in axotomized facial nucleus (axotFN), microglia were isolated from explant culture of axotFN according to a previously reported method (Nakajima *et al.* 2006). Three days after transection, the facial nuclei were cut out from the brainstem and minced under aseptic conditions. The minced pieces were cultured in wells of a 12-well plate as explant culture for 24 h with Dulbecco's modified Eagle's medium (DMEM) containing 10% fetal bovine serum (FBS), and the tissue pieces were removed. The adhered microglia were further maintained with DMEM containing 10% FBS for 5 days and recovered as axotFN-microglia. All of the cells were Iba1-positive.

For the experiment regarding M-CSF neutralization, both left and right facial nerves of adult rats were cut, and 3 days later left and right facial nuclei were separately cultured on one well of a 24-well plate as explant culture with DMEM containing 10% FBS. After

24 h, the tissue pieces in each well were removed by rinsing adhered microglia with serum-free DMEM four times, and left facial nucleus-derived microglia and right facial nucleus-derived microglia were exposed to serum-free DMEM containing normal goat IgG (1.0 μg/mL) and serum-free DMEM containing M-CSF neutralizing goat IgG (1.0 μg/mL), respectively. One hour later, the cell number in each well was determined (defined as 1 day). Subsequently, the media of left and right facial nucleus-derived microglial cultures

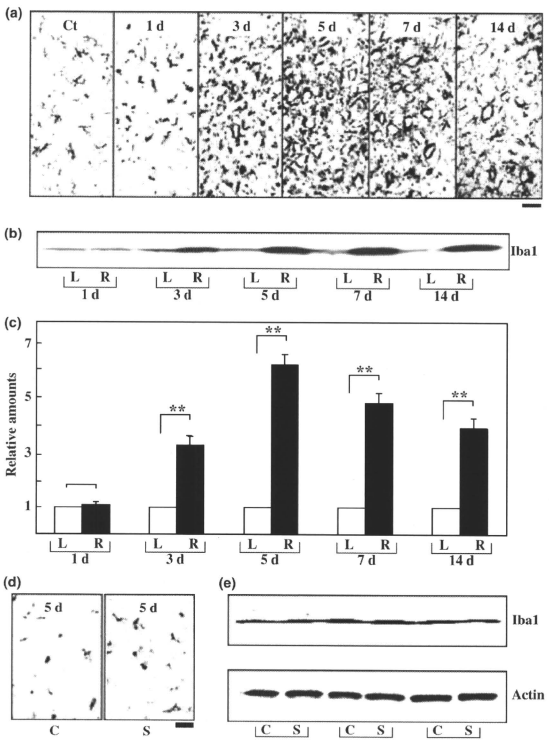

Fig. 1 Microglial response. (a) immunohistochemical observation. The right facial nerve of adult rats was transected, and brains were removed at 1, 3, 5, 7, and 14 days following transection. The right facial nucleus of the brainstem was immunohistochemically stained by CD11b antibody, as described in the Materials and Methods. The left facial nucleus was used as the control (Ct). Representative photos are shown. Scale bar = 50 μm. (b) Immunoblot analyses. The right facial nerve of adult rat was cut, and the brains were removed at 1, 3, 5, 7, and 14 days after transection. The right (R) and left (L) facial nuclei of each rat were cut out, respectively, and were homogenized, as described in the Materials and Methods. Each homogenate was immunoblotted for Iba1. The representative result is shown. (c) Quantification of Iba1. The intensity of the Iba1 band in (b) was determined by densitometer, and the intensity of transected facial nucleus (R) is expressed as a value relative to that of control nucleus (L). The data are indicated as mean ± SD from the experiments using three different rats (**$p < 0.01$). (d) Immunohistochemistry for Iba1 in sham-operated facial nucleus. The right facial nerve of adult rat was sham-operated, and the left one was left without surgery. The brains were removed at 5 days following surgery. The left facial nucleus (C) and right facial nucleus (S) of the brainstem was immunohistochemically stained by Iba1 antibody, as described in the Materials and Methods. Scale bar = 50 μm. (e) Levels of Iba1 and actin in sham-operated facial nucleus. The right facial nerve of three adult rats was sham-operated as above, and after 5 days, left (C) and right (S) facial nuclei of each rat were removed, respectively, and their tissue homogenates were immunoblotted for Iba1 and actin.

were thoroughly replaced with DMEM containing 10% FBS and normal goat IgG (1.0 μg/mL) and DMEM containing 10% FBS and M-CSF neutralizing goat IgG (1.0 μg/mL), respectively. On day 3, half of the medium in each well was replaced with the same fresh medium. The total cell number of microglia in each well was determined under a microscope during 5 days.

Preparation of microglia from neonatal rat brain-derived primary culture

To analyze the effects of M-CSF on microglial proliferation *in vitro*, microglia from neonatal rat brain-derived primary culture (neo-primary microglia) were prepared as described previously (Nakajima *et al.* 2002). The purity of the microglia was estimated to be

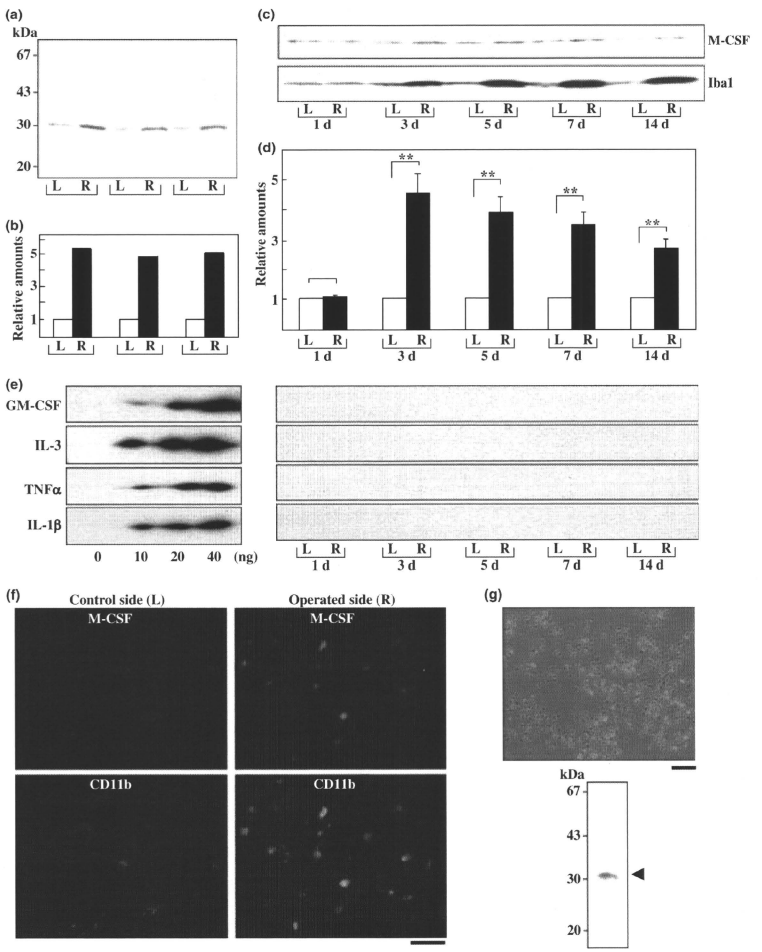

99.9–100% based on their Iba1 immunoreactivity, as described previously (Nakajima *et al.* 2001).

For the assay of proliferation, neo-primary microglia were seeded on the wells of a 24-well plate (Nunclon, Roskilde, Denmark) at a density of 2.0×10^4/well. The microglia were exposed to M-CSF (0–40 ng/mL), and at a suitable time point (0–5 days), the cell number in the wells was directly determined under a microscope. In each well, four fields of 1 mm^2 were chosen for the counting.

To examine the effects of M-CSF on the induction of cFms or on the procession of the cell cycle (expression of PCNA protein), neo-primary microglia were seeded on 60-mm dishes (Nunclon) at a density of 2.0×10^6/dish. The dishes were rinsed three times with serum-free Dulbecco's modified Eagle medium and maintained with the same medium overnight. The microglia were stimulated with M-CSF (0–40 ng/mL) and maintained for 0–24 h. At the end of the incubation period, the microglia were collected by rubber policeman, which is a glass stick with a rubber surface that can scrape cells adhered to the surface of plastic dishes. The recovered cells were freeze-dried.

Immunoblotting

For the analysis of Iba1, M-CSF, GM-CSF, IL-3, TNFα, IL-1β, cFms, PCNA, and actin in the facial nucleus or cultured microglia, the recovered facial nucleus, or collected microglia were solubilized by sonication with non-reducing Laemmli's sample solution [62.5 mM Tris–HCl (pH 6.8), 2% sodium dodecyl sulfate, and 5% glycerol] and centrifuged at 100 000 *g* for 30 min. An aliquot of the supernatant was taken for protein determination (Lowry *et al.* 1951). The remaining supernatant was adjusted to contain 2.5% 2-mercaptethanol and was heated at 90°C for 3 min.

The resultant samples were subjected to immunoblotting, as reported previously (Nakajima *et al.* 2002). The blotted Immobilon (Millipore Corporation, Bedford, MA, USA) was incubated with primary antibody (1 : 1000 for Iba1 and actin, 1 : 200 for M-CSF, GM-CSF, IL-3, TNFα, IL-1β, cFms, and PCNA) at 4°C overnight. After the membrane was rinsed five times, it was incubated with HRP-conjugated anti-rabbit IgG antibody (1 : 1000), HRP-conjugated anti-goat IgG antibody (1 : 1000), or HRP-conjugated anti-mouse IgG antibody (1 : 1000) for 1 h at 25°C. After sufficient rinsing, the antigen-antibody complex on the membrane was detected with an ELC chemiluminescence system. If necessary, the membranes were re-probed.

Statistical analysis

The densities of the bands of Iba1, M-CSF, cFms, PCNA, and actin detected in the immunoblotting were measured by densitometer. The results are expressed as the means ± SD from experiments using three different rats or at least three different lots of cells. Differences between the contralateral and ipsilateral nucleus or between the control and stimulated microglia were assessed via Student's *t*-test. In all cases, *p*-values of less than 0.05 were considered significant ($*p < 0.05$, $**p < 0.01$).

Results

Microglial proliferation in axotomized rat facial nucleus

We confirmed that the transection of facial nerve causes microglia to increase their numbers in the ipsilateral nucleus, as previously reported (Graeber *et al.* 1998). As shown in Fig. 1(a), immunohistochemical analysis revealed that the number of CD11b-positive microglia increased 3–14 days following transection. In fact, the immunoblotting results indicated that the amounts of Iba1 (a marker of microglia) on the axotomized side were elevated 3–14 days after transection (Fig. 1b), suggesting that microglia were activated and that their cell numbers were enhanced. In the quantitative analysis, the ratio of Iba1 in injured nucleus to that in control nucleus began to increase at 3 days and was maintained at high levels at 5–14 days after transection (Fig. 1c).

The influence of the sham operation was examined, and the results are shown in Fig. 1(d and e). Microglia were immunohistochemically stained with anti-Iba1 antibody in

Fig. 2 Determination of M-CSF in the axotomized facial nucleus. (a) Comparison of M-CSF levels between the control and axotomized sides. The right facial nerve of three adult rats was transected, and after 3 days, right (R) and left (L) facial nuclei of each rat were removed, respectively, and their homogenates were immunoblotted for M-CSF. (b) Quantification of M-CSF. The intensity of the M-CSF band in (a) was determined by densitometer, and the intensity of transected facial nucleus (R) is expressed as a value relative to that of control nucleus (L). (c) Post-traumatic change in M-CSF levels. The right facial nerve of adult rats was transected, and after 1, 3, 5, 7, and 14 days, right (R) and left (L) facial nuclei were removed, and their homogenates were immunoblotted for M-CSF. The representative profile is shown. The Iba1 profile of the same sample is also shown. (d) Quantification of M-CSF levels. The intensity of the M-CSF band in (c) was determined by densitometer, and the value of transected facial nucleus (R) is expressed as a value relative to the control side (L). The data are indicated as mean ± SD from the experiments using three different rats ($**p < 0.01$). (e) Changes in GM-CSF, IL-3, TNFα, and IL-1β levels after transection. The right facial nerve of adult rats was transected, and after 1, 3, 5, 7, and 14 days, right (R) and left (L) facial nuclei were removed, and their homogenates were immunoblotted for GM-CSF, IL-3, TNFα, and IL-1β. The experiments were carried out at least three times. The reactivities of each antibody against each authentic sample (0–40 ng/lane) are shown for each left side. The representative profile is also shown. (f) Immunohistochemistry for M-CSF. The right facial nerve of adult rats was transected, and after 3 days, right (operated side) and left (control side) facial nuclei of the brainstem sections were stained dually with anti-M-CSF antibody and CD11b antibody, as described in the Materials and Methods. The presence of M-CSF and CD11b was visualized by Alexa Fluor 568 (red) and FITC (green), respectively. Representative photos are shown. Scale bar = 50 μm. (g) M-CSF in axotomized facial nucleus-derived microglia. Microglia derived from axotomized facial nucleus were maintained in culture for 5 days, as described in the Materials and Methods. The typical image is shown in the upper panel. Scale bar = 50 μm. The microglia recovered at 5 days were immunoblotted for M-CSF. The representative result is shown in the lower panel.

both left facial nucleus (C; non-operated) and right facial nucleus (S; sham-operated) 5 days after the sham operation. No effects of the sham operation were immunohistochemically observed (Fig. 1d). Immunoblotting also indicated that there was no significant change in the amounts of Iba1 and actin between the two (C and S) sides (Fig. 1e).

Levels of microglial mitogens

The phenomenon noted above raised the possibility that a certain mitogen for microglia participates in the microglial proliferation in transected facial nucleus. To investigate this possibility, we attempted to determine the amounts of candidate mitogens, including M-CSF, GM-CSF and IL-3 (multi-CSF). In a preliminary experiment, we tested the immunoreactivity of these antibodies used in immunoblotting. Each antibody against rat/mouse M-CSF, GM-CSF, and IL-3 detected each authentic mouse CSF (10 ng), respectively, and the band of each mouse CSF was absorbed in the presence of excess amounts of each mouse CSF in our immunoblotting (data not shown), suggesting the sufficient specificity of each antibody.

Next, the amounts of M-CSF in both axotomized and control facial nuclei were determined in three rats whose facial nerves had been cut 5 days previously. Immunoblotting indicated that in three rats, the amounts of M-CSF on the ipsilateral side were significantly higher than those on the contralateral side (Fig. 2a). Approximately fivefold levels of M-CSF were detected on the transected side compared with the control side (Fig. 2b).

Subsequently, the amounts of M-CSF on both sides were compared through 3–14 days after transection. The amounts in the transected facial nucleus appeared to be significantly higher than those in the control nucleus in each set (3, 5, 7, and 14 days) (Fig. 2c). The quantification revealed that the levels of M-CSF peaked at 3 days after transection and that the high levels were maintained for 5–14 days (Fig. 2d). On the other hand, the intensity of Iba1 (a microglial marker), which reflects the microglial cell number, peaked at 5 days after transection (Fig. 2c), as previously shown (Fig. 1c). Thus, analysis of M-CSF on both the transected and control sides clarified that M-CSF is up-regulated in transected facial nucleus.

The amounts of other candidates, GM-CSF and IL-3, were determined in both control and transected facial nucleus. Although each antibody could detect each authentic sample (at least 10 ng), the bands for GM-CSF and IL-3 were not significantly observed in the facial nuclei samples at any time point (Fig. 2e). Likewise, TNFα and IL-1β were not significantly detected on either side (Fig. 2e). In addition, other cytokines (IL-2, IL-4, and IL-5) were not recognized in the facial nucleus samples at all (data not shown). These results strongly suggest that M-CSF is the only mitogen by which microglia proliferate following transection.

Furthermore, we investigated which type of cell produces M-CSF in the injured facial nucleus. Immunohistochemical staining with both CD11b antibody (microglial marker) and M-CSF antibody showed that small amounts of M-CSF proteins were present in microglia in control facial nucleus (Fig. 2f, left side), while these proteins were highly expressed in activated microglia in transected facial nucleus (Fig. 2f, right side). This immunohistochemical result supports the earlier immunoblotting results (Fig. 2a and c).

In addition, to confirm that microglia in the transected facial nucleus contain M-CSF, axotFN-microglia were prepared. The morphology of axotFN-microglia appears to be homogeneous, resembling neo-primary microglia (Fig. 2g, upper panel). Immunoblotting of the cell homogenate for M-CSF revealed that M-CSF proteins are present in the proliferating axotFN-microglia (Fig. 2g, lower panel). This result also agrees with the above immunohistochemical evidence (Fig. 2f).

Levels of cFms (specific receptors of M-CSF)

We next examined the levels of M-CSF receptor (cFms) in the transected facial nucleus. The amounts of cFms in the transected facial nucleus increased abundantly 3–5 days after transection (Fig. 3a). The quantitative analysis indicated that cFms amounts reached a maximal level at 5 days after transection, and that these levels subsequently remained high (Fig. 3b).

To identify the cell type expressing cFms in transected facial nucleus, the transected facial nucleus was stained dually with anti-cFms antibody and microglial marker CD11b (Fig. 3c). The immunohistochemical analysis revealed that all of the cells expressing cFms proteins are microglia (Fig. 3c, upper panels). In contrast, GFAP-expressing astrocytes were not stained by anti-cFms antibody (Fig. 3c, lower panels). These results suggested that microglia up-regulate cFms in the axotomized facial nucleus, thereby initiating a change to the proliferative stage.

Levels of PCNA (an S-phase specific marker)

To investigate whether microglia shift to the mitotic stage when M-CSF/cFms levels are elevated, we analyzed the amounts of PCNA as a marker of proliferation in the transected facial nucleus. PCNA was rapidly induced in the ipsilateral nucleus 3 days after injury (Fig. 3d). The quantitative analysis indicated that the amounts of PCNA peaked at 3 days after transection and then decreased thereafter (Fig. 3e). Iba1 in the same samples increased for 5–7 days after transection with a different transition profile of PCNA (Fig. 3d).

We carried out an immunohistochemical experiment to identify PCNA-expressing cells in the transected facial nucleus. The dual-staining method using anti-PCNA antibody and anti-Iba1 antibody indicated that all of the

PCNA-positive cells were Iba1-positive, indicating that the DNA-replicating cells were all microglia (Fig. 3f, upper panels). In contrast, no GFAP-positive astrocytes corresponded to the PCNA-positive nucleus (Fig. 3f, lower panels). Thus, we clarified that microglia alone replicate DNA and proliferate in the transected facial nucleus.

M-CSF as a mitogen for microglia *in vitro*

As M-CSF was identified as an *in vivo* mitogen for microglia, the effects on the proliferation were investigated by using neo-primary microglia. The isolated neo-primary microglia were not essentially proliferative. However, the microglia responded to the added M-CSF and began to proliferate. The

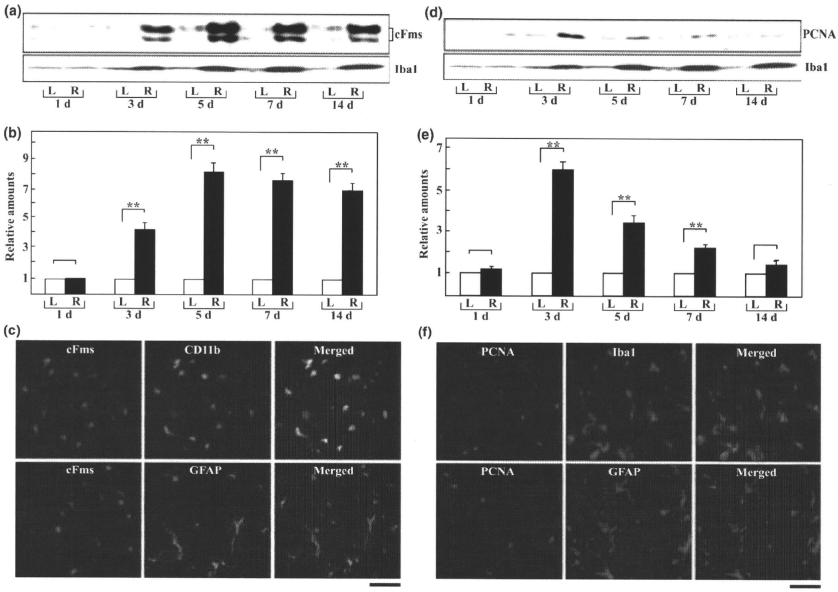

Fig. 3 Determination of cFms and PCNA in the axotomized facial nucleus. (a) Time-course analysis of cFms levels. The right facial nerve of adult rats was transected, and the right (R) and left (L) facial nuclei of each rat were removed at 1, 3, 5, 7, and 14 days following transection. Each set of facial nuclei was immunoblotted for cFms. The results of Iba1 are also shown. (b) Quantification of cFms. The intensity of the cFms band in (a) was determined by densitometer, and the intensity of transected facial nucleus (R) is expressed as a value relative to that of control nucleus (L). The data are indicated as mean ± SD from the experiments using three different rats (**$p < 0.01$). (c) Dual staining with cFms/CD11b antibodies and with cFms/GFAP antibodies. The cryostat sections of the brainstem that were prepared 5 days after transection of facial nerve were stained dually with cFms/CD11b antibodies (upper panels) or with cFms/GFAP antibodies (lower panels), as described in the Materials and Methods. cFms and CD11b were visualized by Alexa Fluor 568 (red) and FITC (green), respectively, and these two pictures were merged (upper panels). In contrast, cFms and GFAP were visualized by Alexa Fluor 568 (red) and Alexa Fluor 488 (green), respectively, and these pictures were also merged (lower panels). Scale bars = 50 μm. (d) Time course of PCNA expression. The right facial nerve of adult rats was transected, and right and left facial nuclei were removed from the brainstem at 1, 3, 5, 7, and 14 days following transection. The tissue homogenate of each facial nucleus was analyzed for PCNA in immunoblotting. The profile of Iba1 is also shown. (e) Quantification of PCNA. The intensity of the PCNA band in A was determined by densitometer, and the intensity of transected facial nucleus (R) is expressed as a value relative to that of control nucleus (L). The data are indicated as mean ± SD from the experiments using three different rats (**$p < 0.01$). (f) Immunohistochemistry for PCNA. The cryosections of the brainstem prepared 3 days after transection were stained dually with PCNA antibody and Iba1 antibody (upper panels) or PCNA antibody and GFAP antibody (lower panels), as described in the Materials and Methods. PCNA and Iba1 were visualized by Alexa Fluor 488 (green) and rhodamine (red), respectively, and these two pictures were merged (upper panels). PCNA and GFAP were also visualized by Alexa Fluor 488 (green) and Alexa Fluor 568 (red), respectively, and these pictures were merged (lower panels). Scale bars = 50 μm.

effects of M-CSF appeared in a dose-dependent manner (0–40 ng/mL) (Fig. 4a). In fact, the cell number increased fourfold with the addition of M-CSF (40 ng/mL) (Fig. 4b). The time-course experiment indicated that the cell number of M-CSF-stimulated microglia began to increase after a 2-day delay (Fig. 4c).

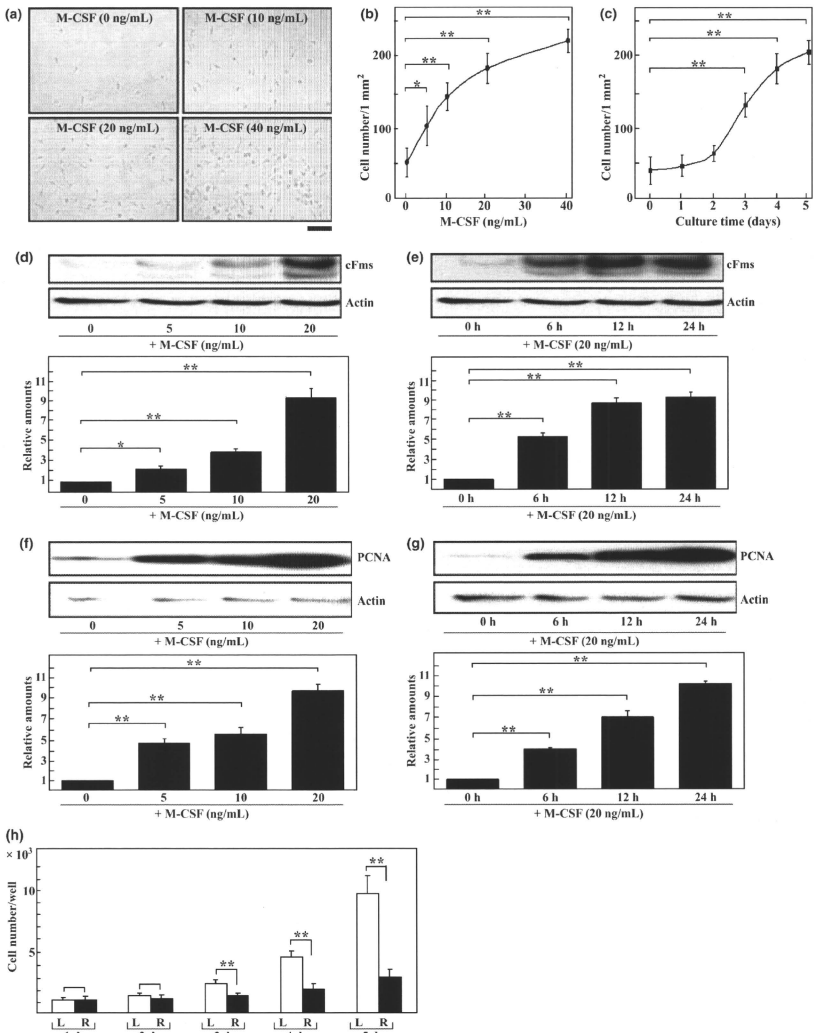

Induction of cFms by treatment with M-CSF

As presented above, neuronal injury was found to up-regulate M-CSF, cFms, and PCNA levels in ipsilateral facial nucleus. We presumed that M-CSF allows microglia to induce cFms proteins for the proliferation, because the levels of M-CSF tended to up-regulate earlier than those of cFms (Figs 2d and 3b). This possibility was examined by using neo-primary microglia *in vitro*. M-CSF stimulation significantly induced cFms in microglia depending on the dose of M-CSF (Fig. 4d). The amounts of actin, as an internal control, were almost identical among these microglia. The effects of M-CSF on the induction of cFms were also culture time-dependent (Fig. 4e). The amounts of actin did not significantly change. Thus, M-CSF was proven to induce cFms in neo-primary microglia.

Up-regulation of PCNA by treatment with M-CSF

As M-CSF was thought to shift microglia to the proliferative stage by advancing the cell cycle, we analyzed the amounts of PCNA in neo-primary microglia stimulated with M-CSF *in vitro*. The amounts of PCNA in microglia increased depending on the dose of M-CSF, while those of actin did not (Fig. 4f). The effects of M-CSF on enhancing PCNA levels were also culture-time dependent (Fig. 4g). Thus, M-CSF was demonstrated to advance the cell cycle to S-phase in neo-primary microglia.

Effects of M-CSF neutralizing antibody on the proliferation of axotFN-microglia

To confirm that M-CSF is actually associated with microglial proliferation in axotFN, we examined whether M-CSF neutralizing antibody (IgG) inhibits the proliferation of axotFN-microglia.

In a preliminary experiment, the antibody was found to recognize at least 5 ng of mouse M-CSF in immunoblotting (data not shown). The isolated axotFN-microglia were shown to increase their number during the culture (Fig. 4h, left side), as described previously (Nakajima *et al.* 2006). However, the addition of M-CSF neutralizing antibody to axotFN-microglia led to a significant suppression of the proliferation which would otherwise have proceeded (Fig. 4h, right side). These results suggest that microglial proliferation occurring in transected facial nucleus is mediated by M-CSF produced/secreted from the microglia themselves.

Fig. 4 Effects of M-CSF on the cell proliferation and on the induction of cFms and PCNA *in vitro*. (a) Effects of M-CSF to proliferate microglia. Neo-primary microglia were treated with M-CSF (0, 10, 20, and 40 ng/mL), respectively, and after 4 days each well was observed under the microscope. (b) Quantitative analysis; dose-dependency of M-CSF. Neo-primary microglia were treated with M-CSF (0, 5, 10, 20, and 40 ng/mL), respectively, and after 4 days the cell number was counted in four square fields of 1 mm^2, which were selected around the center of a well and expressed as the average. The results are expressed as mean ± SD from the experiments using three different lots of microglia. (c) Quantitative analysis; time course experiment. Neo-primary microglia were treated with M-CSF (20 ng/mL) for 0, 1, 2. 3, 4, and 5 days, and the cell number, which is expressed as an average, was determined in four square fields of 1 mm^2 selected around the center of a well. The results are expressed as mean ± SD from the experiments using three different lots of microglia. (d) Effects of M-CSF on the induction of cFms; dose-dependency. Neo-primary microglia were prepared and stimulated with M-CSF (0, 5, 10, and 20 ng/mL). These cultures were maintained for 24 h, and cFms proteins in each culture were determined by immunoblotting. Actin was analyzed in the same microglial cultures. A typical profile is shown in the upper panels. The intensities of the bands of cFms and actin were determined by densitometer, and the amounts of cFms are expressed as values relative to those of actin. The data are indicated as the mean ± SD from the experiments using three different lots of microglia (lower panel) (*$p < 0.05$, **$p < 0.01$). (e) Effects of M-CSF on the induction of cFms; time course. Neo-primary microglia were prepared and stimulated with M-CSF (20 ng/mL) for 0, 6, 12, and 24 h, respectively. The amounts of cFms proteins in each culture were determined by immunoblotting. Actin was analyzed in the same microglial cultures. A typical profile is shown in the upper panels. The intensities of bands of cFms and actin were determined by densitometer, and the amounts of cFms are expressed as values relative to those of actin. The data are indicated as the mean ± SD from the experiments using three different lots of microglia (lower panel) (**$p < 0.01$). (f) Effects of M-CSF on transition of the cell cycle to S-phase; dose-dependency. Neo-primary microglia were prepared and stimulated with M-CSF (0, 5, 10, and 20 ng/mL). After 24 h, PCNA proteins in each culture were determined by immunoblotting. Actin was analyzed in the same microglial cultures. A typical profile is shown in the upper panels. The intensities of the bands of PCNA and actin were determined by densitometer, and the amounts of PCNA are expressed as values relative to those of actin. The data are indicated as mean ± SD from the experiments using three different lots of microglia (lower panel) (**$p < 0.01$). (g) Effects of M-CSF on transition of the cell cycle to S-phase; time course. Four neo-primary microglial cultures were prepared and stimulated with M-CSF (20 ng/mL) for 0, 6, 12, and 24 h, respectively. PCNA proteins in each culture were determined by immunoblotting. Actin was analyzed in the same microglial cultures. A typical profile is shown in the upper panels. The intensities of bands of PCNA and actin were determined by densitometer, and the amounts of PCNA are expressed as values relative to those of actin. The data are indicated as the mean ± SD from the experiments using three different lots of microglia (**$p < 0.01$). (h) Effects of M-CSF neutralizing antibody on axotomized facial nucleus-derived microglia. Axotomized facial nucleus-derived microglial cultures were prepared, as described in the Materials and Methods. On day 1, left facial nucleus-derived microglia (L) were exposed to medium containing normal goat IgG (1.0 μg/mL), while right facial nucleus-derived microglia (R) were exposed to medium containing M-CSF neutralizing goat IgG (1.0 μg/mL), as described in the Materials and Methods. On day 3, half of the medium in each well was replaced with the same medium. The cell number in each well was determined during 5 days. The data are indicated as the mean ± SD from the experiments using five different rats.

Discussion

One of the microglial features *in vivo* is proliferation in pathological and injured brains, including those affected by Alzheimer's disease (McGeer *et al.* 1993), Parkinson's disease (Członkowska *et al.* 2002), and axotomy (Kreutzberg 1996). Generally, increases in microglial cell numbers have been discussed from the perspective of a progression of disorders. The increased amounts of microglia have been believed to facilitate the progression of diseases in already damaged tissue through the elevated production of harmful factors. To protect neurons from serious damage in the diseased or injured brain, it is important to determine the accurate molecular mechanism for microglial proliferation. For the analysis, we used the rat facial nerve transection model, which is superior to other models in that the remote lesion leaves the blood brain barrier unaffected (Streit *et al.* 1988). Because of this advantage, the microglial proliferation can be seen in the absence of extrinsic hematogenous cells, allowing the increase in microglial cell number in the ipsilateral facial nucleus to be attributed to the resident microglial cells (Graeber *et al.* 1988; Kreutzberg 1996).

What kind of mitogen is involved in the microglial proliferation in axotFN has remained as interesting question. Previous reports have suggested that various types of mitogens, including M-CSF, GM-CSF, IL-3 (Giulian and Ingleman 1988), TNFα, and IL-1β (Ganter *et al.* 1992) may be involved in microglial proliferation *in vivo*. Among them, M-CSF has been highlighted as a major mitogen *in vivo* based on an analysis of osteopetrotic mouse (M-CSF deficient mouse) (Raivich *et al.* 1994). However, the actual amounts of M-CSF in axotFN remain to be determined. In the present study, a line of experiments indicated that M-CSF is up-regulated in microglia in axotFN (Fig. 2a, c, d, f). This consequence is also supported by the results showing that axotFN-microglia contain M-CSF protein (Fig. 2g). Accordingly, it is evident that microglia are major cells producing M-CSF in axotFN. In another injury paradigm, however, neurons have been reported to produce M-CSF (Takeuchi *et al.* 2001), leaving the possibility that plural cell types are engaged in M-CSF production *in vivo*.

Granulocyte macrophage-colony stimulating factor (Hao *et al.* 1990; Ohno *et al.* 1990; Thery *et al.* 1990), IL-3, and other cytokines have also been considered to be possible microglial mitogens *in vivo*. However, as shown in Fig. 2(e), GM-CSF, IL-3, and cytokines (TNFα and IL-1β) were not significantly detected in either control or transected facial nucleus. Consequently, the contribution of GM-CSF, IL-3, TNFα, and IL-1β to microglial proliferation in axotFN might be quite small, if any.

The specific receptor of M-CSF, cFms, was actually measured in axotFN using immunoblotting. The amounts of cFms increased rapidly at 3 days after injury, and these levels were sustained for over 7 days (Fig. 3b), showing a similar profile to the previous reports by Raivich *et al.* (1991), who used the [^{125} I] M-CSF binding method. In addition, the cells expressing cFms proteins were immunohistochemically identified as microglia (Fig. 3c). These results suggest that up-regulation of M-CSF and cFms is closely associated with the microglial proliferation observed in the axotFN.

As we noticed that M-CSF increased earlier than cFms in a time-course experiment (Figs 2d and 3b), a hypothesis that M-CSF allows microglia to induce cFms proteins was tested *in vitro*. The amounts of cFms were promoted in neo-primary microglia by the addition of M-CSF, with the levels depending on the dose of M-CSF and the culture time (Fig. 4d and e). The signals from activated cFms in M-CSF-stimulated microglia would elicit the transcription of cFms gene, followed by the production of cFms proteins.

Proliferating cell nuclear antigen, which is expressed in the nucleus at S-phase, was quickly induced in the ipsilateral nucleus at 3 days after transection and then subsequently decreased (Fig. 3e). The PCNA-positive cells were identified as microglia, but not astrocytes. Thus, at 3 days after transection, a number of microglia turned to the mitotic stage. The possibility that M-CSF advances the cell cycle in microglia was then investigated using neo-primary microglia. The effects of M-CSF in an *in vitro* system (Fig. 4d–g) suggested that up-regulated M-CSF induces cFms in microglia and that the switched microglia become proliferative with the expression of PCNA protein in axotFN.

Then, to demonstrate that M-CSF is actually associated with microglial proliferation in the axotFN, we carried out an M-CSF neutralization experiment (Fig. 4h). The treatment of axotFN-microglia with neutralizing antibody significantly reduced the proliferation of microglia (Fig. 4h). The results clearly indicate that M-CSF secreted from microglia contributes to the microglial proliferation.

Little is known regarding what kinds of stimuli transmit signals for microglial proliferation from injured neurons to microglia in transected facial nucleus. Investigations are therefore required to clarify the mechanism of intercellular interactions between injured neurons and microglia, and to identify trigger molecules to up-regulate M-CSF in microglia.

Taken together, we have demonstrated that M-CSF levels are elevated at the beginning of microglial proliferation in the transected facial nucleus, and that M-CSF induces cFms in microglia and prompts microglia to become proliferative.

Acknowledgements

This work was supported by a Grant-in-Aid for Scientific Research (C) from the Japan Society for the Promotion of Science.

References

Członkowska A., Kurkowska-Jastrzebska I., Członkowski A., Peter D. and Stefano G. B. (2002) Immune processes in the pathogenesis of Parkinson's disease – a potential role for microglia and nitric oxide. *Med. Sci. Monit.* **8**, RA165–RA177.

Dickson D. W., Lee S. C., Mattiace L. A., Yen S.-H. C. and Brosnan C. F. (1993) Microglia and cytokines in neurological disease, with special reference to AIDS and Alzheimer's disease. *Glia* **7**, 75–83.

Ganter G., Northoff H., Männel D. and Gebicke-Härter P. J. (1992) Growth control of cultured microglia. *J. Nerurosic. Res.* **33**, 218–230.

Gehrmann J. and Kreutzberg G. W. (1992) Monoclonal antibodies against macrophages/microglia: immunocytochemical studies of early microglial activation in experimental neuropathology. *Clin. Neuropathol.* **12**, 301–306.

Giulian D. and Ingleman J. E. (1988) Colony-stimulating factors as promoters of ameboid microglia. *J. Neurosci.* **8**, 4707–4717.

Giulian D., Chen J., Ingleman J. E. and Noponen M. (1989) The role of mononuclear phagocytes in would healing after traumatic injury to adult mammalian brain. *J. Neurosci.* **9**, 4416–4429.

Graeber M. B., Streit W. J. and Kreutzberg G. W. (1988) Axotomy of the rat facial nerve leads to increased CR3 complement receptor expression by activated microglial cells. *J. Neurosci. Res.* **21**, 18–24.

Graeber M. B., Lopez-Redondo F., Ikoma E., Ishikawa M., Imai Y., Nkajima K., Kreutzberg G. W. and Kohsaka S. (1998) The microglia/macrophage response in the neonatal rat facial nucleus following axtomy. *Brain Res.* **813**, 241–253.

Hao C., Guilbert L. J. and Fedoroff S. (1990) Production of colony stimulating factor-1 (CSF-1) by mouse astroglia in vitro. *J. Neurosci. Res.* **27**, 314–323.

Imai Y., Ibata I., Ito D., Ohsawa K. and Kohsaka S. (1996) A novel gene iba1 in the major histocompatibility complex class III rerion encoding an EF hand protein expressed in a monocytic lineage. *Biochem. Biophys. Res. Commun.* **224**, 855–862.

Kato H., Takahashi A. and Itoyama Y. (2003) Cell cycle protein expression in proliferating microglia and astrocytes following transient global cerebral ischemia in the rat. *Brain Res. Bull.* **60**, 215–221.

Kreutzberg G. W. (1996) Microglia: a sensor for pathological events in the CNS. *Trends Neurosci.* **19**, 312–318.

Lassmann H., Vass K., Brunner C. H. and Seitelberger F. (1986) Characterization of inflammatory infiltrates in experimental allergic encephalomyelitis. *Prog. Neuropathol.* **6**, 33–62.

Lee S. C., Liu W., Brosnan C. F. and Dickson D. W. (1994) GM-CSF promotes proliferation of human fetal and adult microglia in primary cultures. *Glia* **12**, 309–318.

Liva S. M. and de Vellis J. (2001) IL-5 induces proliferation and activation of microglia via an unknown receptor. *Neurochem. Res.* **26**, 629–637.

Lowry O. J., Rosebrough N. J., Farr A. L. and Randall R. J. (1951) Protein measurement with the Folin phenol reagent. *J. Biol. Chem.* **193**, 265–275.

McGeer P. L., Kawamata T., Walker D. G., Akiyama H., Tooyama I. and McGeer E. G. (1993) Microglia in degenerative neurological disease. *Glia* **7**, 84–92.

Nakajima K., Reddington M., Kohsaka S. and Kreutzberg G. W. (1996) Induction of urokinase-type plasminogen activator in rat facial nucleus by axotomy of the facial nerve. *J. Neurochem.* **66**, 2500–2505.

Nakajima K., Honda S., Tohyama Y., Imai Y., Kohsaka S. and Kurihara T. (2001) Neurotrophin secretion from cultured microglia. *J. Neurosci. Res.* **65**, 322–331.

Nakajima K., Tohyama Y., Kohsaka S. and Kurihara Y. (2002) Ceramide activates microglia to enhance the production/secretion of brain-derived neurotrophic factor (BDNF) without induction of deleterious factors in vitro. *J. Neurochem.* **80**, 697–705.

Nakajima K., Greaber M. B., Sonoda M., Tohyama Y., Kohsaka S. and Kurihara T. (2006) In vitro proliferation of axotomized rat facial nucleus-derived activated microglia in an autocrine fashion. *J. Neurosci. Res.* **84**, 348–359.

Nelson P. T., Soma L. A. and Lavi E. (2002) Microglia in diseases of the central nervous system. *Ann. Med.* **34**, 491–500.

Ohno K., Suzumura A., Sawada M. and Marunouchi T. (1990) Production of granulocyte/macrophage colony-stimulation factor by cultured astrocytes. *Biochem. Biophys. Res. Commun.* **169**, 719–724.

Raivich G., Gehrmann J. and Kreutzberg G. W. (1991) Increase of macrophage colony-stimulating factor and granulocyte-macrophage colony-stimulating factor receptors in the regenerating rat facial nucleus. *J. Neurosci. Res.* **30**, 682–686.

Raivich G., Moreno-Flores M., Moller J. C. and Kreutzberg G. W. (1994) Inhibition of posttraumatic microglial proliferation in a genetic model of macrophage colony-stimulating factor deficiency in the mouse. *Eur. J. Neurosci.* **6**, 1615–1618.

Ringheim G. E. (1995) Mitogenic effects of interleukin-5 on microglia. *Neurosci. Lett.* **201**, 131–134.

Sawada M., Suzumura A., Yamamoto H. and Maranouchi T. (1990) Activation and proliferation of isolated microglia by colony stimulating factor-1 and possible involvement of protein kinase C. *Brain Res.* **509**, 119–124.

Sawada M., Suzumura A. and Marunouchi T. (1995) Induction of functional interleukin-2 receptor in mouse microglia. *J. Neurochem.* **64**, 1973–1979.

Streit W. J. (2005) Microglial cells, in *Neuroglia*, 2nd Edn (Kettenmann H. and Ransom B. R., eds), pp. 60–71. Oxford University Press, New York.

Streit W. J., Graeber M. B. and Kreutzberg G. W. (1988) Functional plasticity of microglia: a review. *Glia* **1**, 301–307.

Suzumura A., Sawada M., Marunouchi T. and Yamamoto H. (1993) Proliferation of microglia with IL-4. *Neuroimmunology* **1**, 122–123.

Takeuchi A., Miyaishi O., Kiuchi K. and Isobe K. (2001) Macrophage colony-stimulating factor is expressed in neuron and microglia after focal brain injury. *J. Neurosci. Res.* **65**, 38–44.

Thery C., Hetier E., Evard C. and Mallat M. (1990) Expression of macrophage colony-stimulating factor in the mouse brain during development. *J. Neurosci. Res.* **26**, 129–133.

Weinstein D. L., Walker D. G., Akiyama H. and McGeer P. L. (1990) Herpes simplex virus type I infection induces major histocompatibility complex antigen expression on rat microglia. *J. Neurosci. Res.* **26**, 55–65.

Glycobiology vol. 20 no. 12 pp. 1594–1606, 2010
doi: 10.1093/glycob/cwq108
Advance Access publication on July 28, 2010

Novel ganglioside found in adenocarcinoma cells of Lewis-negative patients

Kyoko Shida[2], Hiroaki Korekane[3], Yoshiko Misonou[2], Shingo Noura[4], Masayuki Ohue[4], Hidenori Takahashi[4], Hiroaki Ohigashi[4], Osamu Ishikawa[4], and Yasuhide Miyamoto[1,2]

[2]Department of Immunology, Osaka Medical Center for Cancer and Cardiovascular Diseases, 1-3-2 Nakamichi, Higashinari-ku, Osaka 537-8511, Japan; [3]Department of Disease Glycomics, The Institute of Scientific and Industrial Research, Osaka University, 8-1 Mihogaoka, Ibaraki, Osaka 567-0047, Japan; and [4]Department of Surgery, Osaka Medical Center for Cancer and Cardiovascular Diseases, 1-3-3 Nakamichi, Higashinari-ku, Osaka 537-8511, Japan

Received on April 19, 2010; revised on July 8, 2010; accepted on July 9, 2010

We have precisely analyzed the structures of glycosphingolipids of human cancer cells and normal epithelial cells using several methods, including enzymatic release of carbohydrate moieties, fluorescent labeling, and identification using 2D mapping, enzymatic digestion, and mass spectrometry. These analyses enabled the identification of novel tumor-associated carbohydrate antigens that can be used to elucidate the involvement of carbohydrates in cancer malignancy and could act as candidate tumor markers. In our previous study, we identified a novel glycosphingolipid that accumulates in colon cancer cells, NeuAcα2-6(Fucα1-2)Galβ1-4GlcNAcβ1-3Galβ1-4Glc (α2-6 sialylated type 2H, ST2H). Here, structural analyses of cancer cells and normal epithelial cells from 60 colorectal and five pancreatic cancer patients, including four and two Lewis-negative individuals, respectively, reveal the presence of an additional novel glycosphingolipid, NeuAcα2-6(Fucα1-2)Galβ1-3GlcNAcβ1-3Galβ1-4Glc (α2-6 sialylated type 1H, ST1H). ST2H was found in colorectal and pancreatic cancer cells from about half of the cases. Unlike ST2H, ST1H was found in cancer cells from three out of six Lewis-negative patients (i.e., two cases of colorectal and one case of pancreatic cancer). However, the moiety was not found in normal epithelial cells or cancer cells from 59 Lewis-positive patients. These findings suggest that the accumulation of this carbohydrate antigen occurs predominantly in cancer cells of Lewis-negative patients. When the ST1H epitope is also carried on mucins as well as glycosphingolipids, this epitope is a promising tumor marker candidate, especially for Lewis-negative individuals.

Keywords: colorectal cancer/glycosphingolipid/Lewis type/pancreatic cancer

Introduction

Drastic alterations in glycosphingolipids (GSLs) and glycoproteins have been observed in a variety of human cancers, and many altered carbohydrate determinants, including sialyl Le^x (SLe^x) and sialyl Le^a (SLe^a), are classified as tumor-associated carbohydrate antigens (Hakomori 1989; Hakomori 2002). A subsequent series of studies have indicated the functional significance of tumor-associated carbohydrate antigens in cancer malignancy, such as metastasis and invasion (Fukuda 1996; Hakomori 1996). For example, SLe^a and SLe^x function as ligands for selectins and are thought to be involved in hematogeneous metastasis (Kannagi et al. 2004). Furthermore, tumor-associated carbohydrate determinants have been utilized as useful tumor markers for the diagnosis of cancer (Kannagi et al. 2004). CA19-9, SLe^a epiotope, is one of the most well-known serum tumor markers and is frequently used for clinical diagnosis of a variety of cancers such as pancreatic, colorectal, and stomach cancers. Thus, identification of novel tumor-associated carbohydrate antigens should give important clues concerning the involvement of carbohydrates in cancer malignancy as well as providing potentially useful tumor markers.

We previously identified a novel tumor-associated carbohydrate antigen in the GSLs from human colon cancer, NeuAcα2-6(Fucα1-2)Galβ1-4GlcNAcβ1-3Galβ1-4Glc (α2-6 sialylated type 2H, abbreviated as ST2H), which is an isomer of SLe^a and SLe^x (Korekane et al. 2007). We have analyzed the structures of GSLs derived from colorectal cancer cells and normal colorectal epithelial cells from 16 patients (Misonou et al. 2009). ST2H was found in colorectal cancer cells from half of the cases. Moreover, ST2H was found in colorectal cancer cells from most of the cases of colorectal cancer cells having hepatic metastasis. ST2H was not found in normal epithelial cells from all the 16 cases. A biosynthetic pathway of ST2H is proposed in Figure 4.

It is well known that the histo-blood group-related carbohydrate antigens, ABH and Lewis, are genetically defined (Nishihara et al. 1994; Kudo et al. 1996; Hakomori 1999). Lewis enzyme (also called FUT3) is the only enzyme responsible for the synthesis of Lewis antigens, such as Le^a, Le^b, and SLe^a in vivo (Kukowska-Latallo et al. 1990) (ref, Figure 4). Lewis-negative individuals, who make up approximately 10% of the population, are homozygotes for the inactive Lewis gene alleles (Mollicone et al. 1994; Nishihara et al. 1994; Elmgren et al. 1997). Such individuals do not possess Lewis enzyme activity and never express Le^a, Le^b, and SLe^a in any tissue (Yazawa et al. 1995; Narimatsu et al. 1996; Nishihara et al. 1999).

In order to discover additional tumor-associated carbohydrate antigens, structural analyses of GSLs of cancer cells

[1]To whom correspondence should be addressed: Tel.: +81-6-6972-1181; Fax: +81-6-6972-7749; E-mail: miyamoto-ya@mc.pref.osaka.jp

Table I. Clinicopathological information on the six Lewis-negative patients with colorectal (cases 1–4) or pancreatic adenocarcinoma (cases 5 and 6)

No	Age	Sex	Tumor localization	Tumor size (mm)	Histological differentiation	Depth of invasion	LN*	LM*	Blood type	CEA (ng/mL)	CA19-9 (U/mL)
1	58	F	Sigmoid	55 × 50	Moderate	SE*	N3	H2	O	27.0	0
2	65	M	Transverse	85 × 50	Moderate	SS*	N0	H1	B	17.7	0
3	53	M	Sigmoid	44 × 33	Moderate	SS	N1	H1	A	3.6	0
4	68	M	Rectum	60 × 50	Well	SS	N1	H0	O	1.0	0
5	85	F	Body	22	Well	T3	N0	H0	A	N.D.*	0
6	66	F	Head	24	Well	T3	N1	H0	A	1.4	0

LN, lymph node metastasis; LM, liver metastasis; SE, serosa exposed; SS, subserosa; N.D., not determined.

have been undertaken. We have analyzed samples from 60 colorectal cancer and five pancreatic cancer patients, including four and two genuine Lewis-negative patients, respectively. We have identified a novel tumor-associated carbohydrate antigen. The antigen accumulates chiefly in cancer cells from Lewis-negative individuals and is a promising candidate tumor marker, especially for Lewis-negative individuals.

Results

Determination of Lewis types

The structural analyses of GSLs of cancer cells and normal epithelial cells from 65 cancer patients (60 cases of colorectal cancer and five cases of pancreatic cancer) were carried out. Among the 65 cases, 56 cases of colorectal cancer patients and three cases of pancreatic cancer patients were determined to be Lewis positive. High levels of Le^a and Le^b structures were observed in GSLs of cancer cells and normal epithelial cells from all the Lewis-positive cases with serum values of CA19-9, a SLe^a determinant, of more than 5 U/mL. The other four cases of colorectal cancer patients (cases 1–4) and two cases of pancreatic cancer patient (cases 5 and 6) were determined to be genuine Lewis negative. The incidence of Lewis-negative individuals (six out of 65) is in good agreement with the anticipated frequency in the population (i.e., 10%). The clinicopathological features of the six patients are described in Table I. Le^a structures were either absent or barely detected in GSLs of cancer cells and normal epithelial cells from these six patients. Moreover, serum CA19-9 values of these patients are 0 U/mL (Table I). Genotyping of the Lewis gene and Lewis enzyme activity were also examined. The full open reading frames of the Lewis gene from all six patients were sequenced. All of the six patients were homozygotes of previously reported null Lewis gene alleles. Cases 1–5 possess two point mutations, T59G and G508A, in both alleles (Nishihara et al. 1994). Case 6 was found to possess two point mutations, T59G and G508A, and another two point mutations, T202C and C314T, in each allele (Elmgren et al. 1997). In addition, as predicted, Lewis activity (α1-4 fucosyltransferase) was not detected to any extent in cancer cells as well as normal colorectal and pancreatic cells of the six cases (data not shown).

Structural analysis of pyridylaminated (PA)-oligosaccharides prepared from colorectal and pancreatic adenocarcinoma cells of Lewis-negative patients having novel tumor-associated carbohydrate antigen

We found a novel GSL in the cancer cells from three out of 65 patients (two colorectal and one pancreatic cancer) who were all Lewis-negative individuals (cases 1, 4, and 6 in Table I). This GSL was not found in normal colorectal and pancreatic epithelial cells from any of the 65 cases. Since the structures of the GSLs of the cancer cells from the three patients were very similar, only the structures of GSLs of rectal cancer cells from case 4 and pancreatic cancer cells from case 6 are shown. Figure 1A shows the acidic and neutral PA-oligosaccharides from rectal cancer cells and normal rectal epithelial cells from case 4. Ten peaks (A1–A10) and 12 peaks (N1–N12) were obtained from acidic and neutral GSLs of rectal cancer cells, respectively (Figure 1A, a and c). Each of the peaks was further purified by reversed-phase high-performance liquid chromatography (HPLC). Peak A8 was separated into three major components, and peaks N6, N7, N9, and N10 were each separated into two major components by reversed-phase HPLC. The peaks were designated A8-1, A8-2, A8-3, N6-1, N6-2, N7-1, N7-2, N9-1, N9-2, N10-1, and N10-2 (Figure 1A, a and c). Ten peaks (A1-A8, A11, A12) and 12 peaks (N1-N10, N12, N13) were obtained from acidic and neutral GSLs of normal rectal epithelial cells, respectively (Figure 1A, b and d). Peak A8 of normal rectal epithelial cells comprised one major component, which corresponds to A8-1 of rectal cancer cells (Figure 1A, b). Peaks N6, N7, N9, and N10 of normal rectal epithelial cells were separated into two major components, similar to rectal cancer cells (Figure 1A, d).

Figure 1B shows the acidic and neutral PA-oligosaccharides from pancreatic cancer cells and normal pancreatic epithelial cells from case 6. Eight peaks (A1–A4, A6–A8, A11) and 11 peaks (N1–N9, N12, N14) were obtained from the acidic and neutral GSLs of pancreatic cancer cells, respectively (Figure 1B, a and c). Six peaks (A1, A3, A4, A7, A13, A14) and 10 peaks (N1-N8, N14, N15) were obtained from the acidic and neutral GSLs of normal pancreatic epithelial cells, respectively (Figure 1B, b and d). Peak A8 of case 6 was separated into two major components by reversed-phase HPLC, corresponding to A8-1 and A8-2 of case 4 (Figure 1B, a). The other peaks from the pancreatic cancer and normal pancreatic cells were shown to comprise a single major component by

reversed-phase HPLC. Peaks N6, N7, and N9 corresponded to N6-1, N7-1, and N9-1 of case 4, respectively (Figure 1B, c and d). A comparison was carried out between the positions on the map and the positions of standard PA-oligosaccharides. With the exception of A8-2, all other peaks matched the standard oligosaccharides (data not shown). The structures of the matched oligosaccharides were also confirmed by mass spectrometry. The predicted structures of the acidic and neutral GSLs of cancer cells and normal epithelial cells from cases 4 and 6 are presented in Tables II and III, respectively.

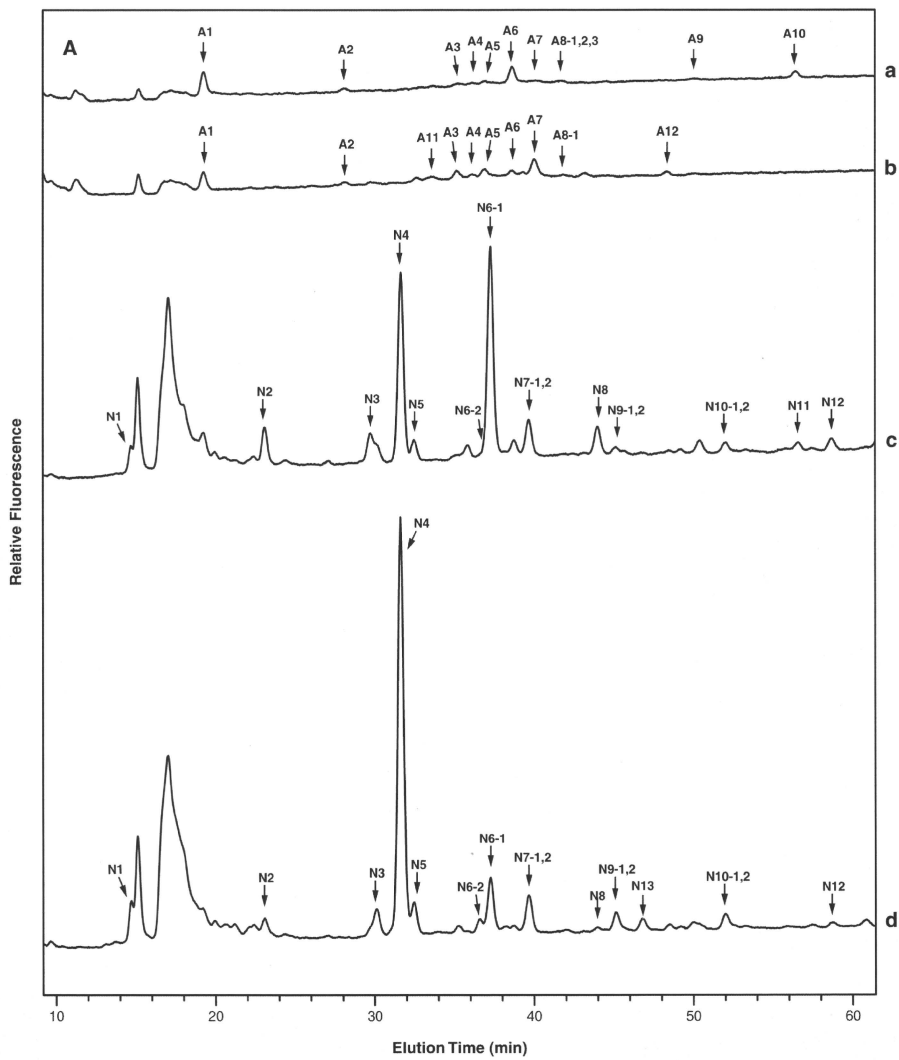

1596

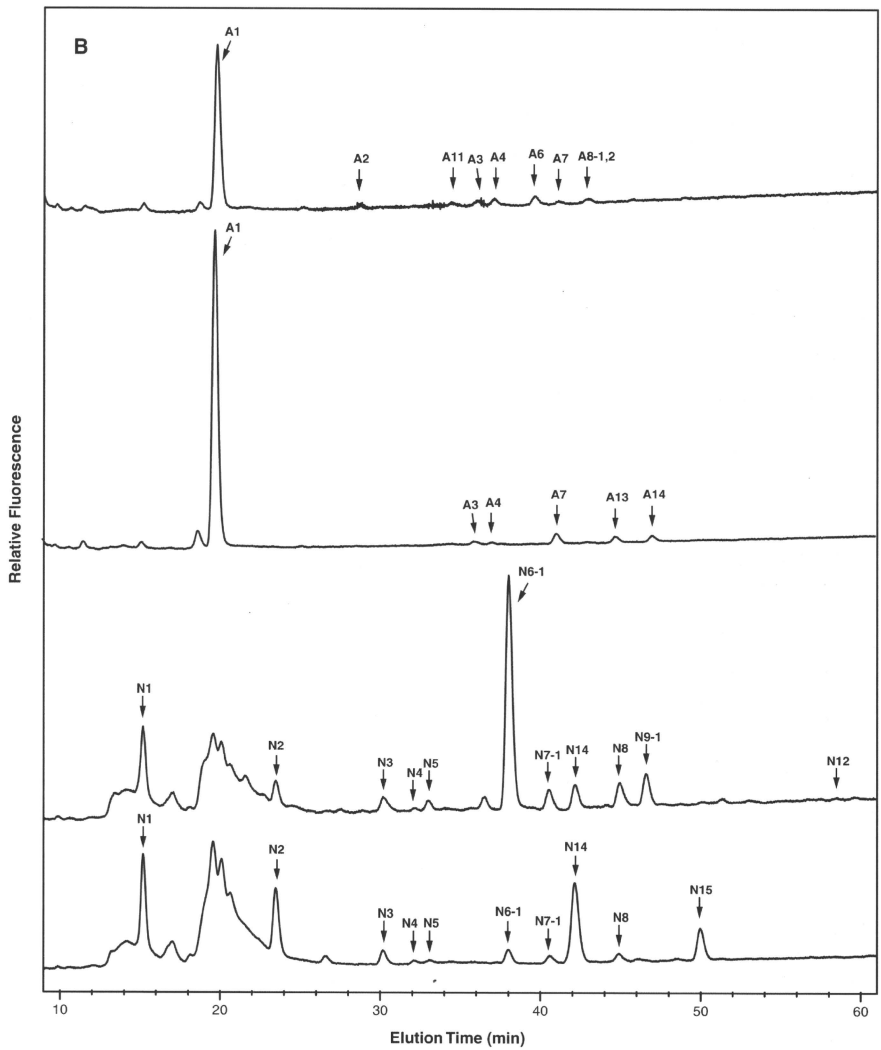

Fig. 1. Size fractionation HPLC of acidic and neutral PA-oligosaccharide mixtures obtained from rectal cancer and normal rectal epithelial cells from case 4 (**A**) and pancreatic cancer and normal pancreatic epithelial cells from case 6 (**B**). **A** and **B**: a, acidic fraction of cancer cells; b, acidic fraction of normal epithelial cells; c, neutral fraction of cancer cells; d, neutral fraction of normal epithelial cells. Identified PA-oligosaccharides in each peak are highlighted with an arrow and numbered with fraction numbers as per Tables II and III. Reverse-phase HPLC separated some of the peaks into two or three components (indicated by the numbers given after the hyphen). Peaks at around 20 min in **A** and **B**, c, and other minor peaks without arrows are artifacts and not PA-oligosaccharides derived from GSLs, as confirmed by mass spectrometry.

The common feature of the profiles of the GSLs from cases 4 and 6 is that Type 1H (N6-1) is greatly increased during carcinogenesis to become the dominant peak (Figure 1A and B, c). This was also observed in the profile of GSLs from case 1. Furthermore, two additional observations regarding the expression of Lewis antigen in Lewis-negative individuals are noteworthy. Firstly, although it is thought that Lewis antigens such as Le^a, Le^b, and SLe^a are not expressed in any tissues of

Table II. Estimated structures of acidic and neutral PA-oligosaccharides from rectal cancer and normal rectal epithelial cells of case 4 (C, cancer cells; N, normal epithelial cells)

Fraction	Structure	Abbreviation	Ratio (%)	
			C	N
acidic				
A1	Neu5Acα2-3Galβ1-4Glc-PA	GM3	3.6	1.7
A2	Neu5Acα2-8Neu5Acα2-3Galβ1-4Glc-PA	GD3	0.3	0.2
A11	Galβ1-3GalNAcβ1-4Galβ1-4Glc-PA 3 Neu5Acα2	GM1	0	0.3
A3	Neu5Acα2-3Galβ1-3GlcNAcβ1-3Galβ1-4Glc-PA	SLe^c	0.5	1.6
A4	Galβ1-3GalNAcβ1-4Galβ1-4Glc-PA 3 3 Neu5Acα2 Neu5Acα2	GD1a	0.2	0.3
A5	Galβ1-3GlcNAcβ1-3Galβ1-4Glc-PA 6 Neu5Acα2	LST-b	0.5	1.2
A6	Neu5Acα2-6Galβ1-4GlcNAcβ1-3Galβ1-4Glc-PA	LST-c	4.9	0.6
A7	Neu5Acα2-3Galβ1-3GlcNAcβ1-3Galβ1-4Glc-PA 6 Neu5Acα2	$IV^3NeuAc\alpha,III^6NeuAc\alpha$-$Lc_4$	0.2	2.3
A8-1	Neu5Acα2-3Galβ1-4GlcNAcβ1-3Galβ1-4Glc-PA 3 Fucα1	SLe^x	0.1	0.1
A8-2	Neu5Acα2-6Galβ1-3GlcNAcβ1-3Galβ1-4Glc-PA 2 Fucα1	ST1H	0.1	0
A8-3	Neu5Acα2-6Galβ1-4GlcNAcβ1-3Galβ1-4Glc-PA 2 Fucα1	ST2H	0.1	0
A12	Galβ1-3GlcNAcβ1-3Galβ1-3GlcNAcβ1-3Galβ1-4Glc-PA 6 Neu5Acα2	$V^6NeuAc\alpha$-Lc_6	0	0.4
A9	Neu5Acα2-6Galβ1-4GlcNAcβ1-3Galβ1-3GlcNAcβ1-3Galβ1-4Glc-PA	$VI^6NeuAc\alpha$-$_{1,2}Lc_6$	0.2	0
A10	Neu5Acα2-6Galβ1-4GlcNAcβ1-3Galβ1-4GlcNAcβ1-3Galβ1-4Glc-PA 3 Fucα1	$VI^6NeuAc\alpha,III^3Fuc\alpha$-$nLc_6$	2.3	0

1598